Agricultural and Forest Meteorology 213 (2015) 10–22

Contents lists available at ScienceDirect

Agricultural and Forest Meteorology

journal homepage: www.elsevier.com/locate/agrformet

How do rubber (*Hevea brasiliensis*) plantations behave under seasonal water stress in northeastern Thailand and central Cambodia?

Tomo'omi Kumagai[a,*], Ryan G. Mudd[b], Thomas W. Giambelluca[b], Nakako Kobayashi[a], Yoshiyuki Miyazawa[c], Tiva Khan Lim[d], Wen Liu[b], Maoyi Huang[e], Jefferson M. Fox[f], Alan D. Ziegler[g], Song Yin[d], Sophea Veasna Mak[d], Poonpipope Kasemsap[h]

[a] Hydrospheric Atmospheric Research Center, Nagoya University, Chikusa-ku, Nagoya 464-8601, Japan
[b] Department of Geography, University of Hawai'i at Mānoa, Honolulu, HI 96822, USA
[c] Research Institute for East Asia Environments, Kyushu University, Motooka, Fukuoka 811-0395, Japan
[d] Cambodian Rubber Research Institute, Phnom Penh, Cambodia
[e] Atmospheric Sciences and Global Change Division, Pacific Northwest National Laboratory, Richland, WA 99352, USA
[f] East-West Center, Honolulu, HI 96848, USA
[g] Department of Geography, National University of Singapore, 117570, Singapore
[h] Department of Horticulture, Faculty of Agriculture, Kasetsart University, Bangkok 10900, Thailand

ARTICLE INFO

Article history:
Received 28 October 2014
Received in revised form 4 June 2015
Accepted 21 June 2015

Keywords:
Tropical deciduous trees
Stomatal control
Transpiration
Water vapor flux
Eddy covariance
Soil moisture

ABSTRACT

Delineating the characteristics of biosphere-atmosphere exchange in rubber (*Hevea brasiliensis* Müll. Arg.) plantations, which are rapidly expanding throughout mainland Southeast Asia, is important to understanding the impacts of the land-use change on environmental processes. In attempt to shed new light on the impacts of conversion to rubber, we have conducted eddy flux measurements over a 3-year period in two rubber plantation sites: (1) Som Sanuk, located in northeastern Thailand; and (2) Cambodian Rubber Research Institute (CRRI), located in central Cambodia. Both sites have a distinct dry season. We used a combination of actual evapotranspiration (E_T) flux measurements and an inverted version of a simple 2-layer E_T model for estimating the mean canopy stomatal conductance (g_s). The potential water balance (precipitation (P) – potential evaporation (E_{T_POT})) for each season (i.e., December–February: DJF, March–May: MAM, June–August: JJA, and September–November: SON) revealed when and how the water use is controlled. In the seasons when actual water balance ($P - E_T$) was negative (DJF and MAM), the deficit was compensated with soil water from the previous season at depths of 0–2 m (Thailand site) and 0–3 m (Cambodia site). At both sites, the reference value of g_s (g_{sref}) and the sensitivity of g_s to atmospheric demand (m) appeared to be less in DJF and MAM than each in the other two 3-month periods (seasons). On average, in a whole year, m/g_{sref} was less in Thailand («0.6) than in Cambodia (near 0.6 for part of the year), suggesting that there was less sufficient stomatal regulation at the Thailand site, where there might be little risk of water stress-induced hydraulic failure because of its higher annual rainfall amount. In comparison, at CRRI where annual $P - E_{T\_POT}$ was negative, there was stricter stomatal regulation, preventing excessive xylem cavitation.

1. Introduction

Rubber (*Hevea brasiliensis* Müll. Arg.) is among the major economic tree crops of tropical areas throughout the world, especially Southeast Asia. Association of Natural Rubber Producing Countries (ANRPC) (2010) estimated that from 2003 to 2010 more than 1,500,000 ha of land were converted to rubber in southern China, Thailand, Vietnam, and Cambodia (see Fig. 1). Rubber is currently expanding rapidly in non-traditional areas of Myanmar, Laos, and India. In the uplands of mainland Southeast Asia, about 9% of the current vegetation, including evergreen broadleaf trees and swidden-related secondary vegetation, is projected to be replaced by tree plantations and diversified farming systems by 2050 (Fox et al., 2012). Almost half of this transition is expected to be due to the expansion of rubber cultivation, the most rapidly expanding tree crop in the region, resulting in a projected fourfold increase in land area devoted to rubber plantation (Fox et al., 2012, 2014).

* Corresponding author at: Hydrospheric Atmospheric Research Center, Nagoya University, Furo-cho, Chikusa-ku, Nagoya, Aichi 464-8601, Japan. Fax: +81 52 788 6206.
E-mail address: tomoomikumagai@gmail.com (T. Kumagai).

http://dx.doi.org/10.1016/j.agrformet.2015.06.011
0168-1923/

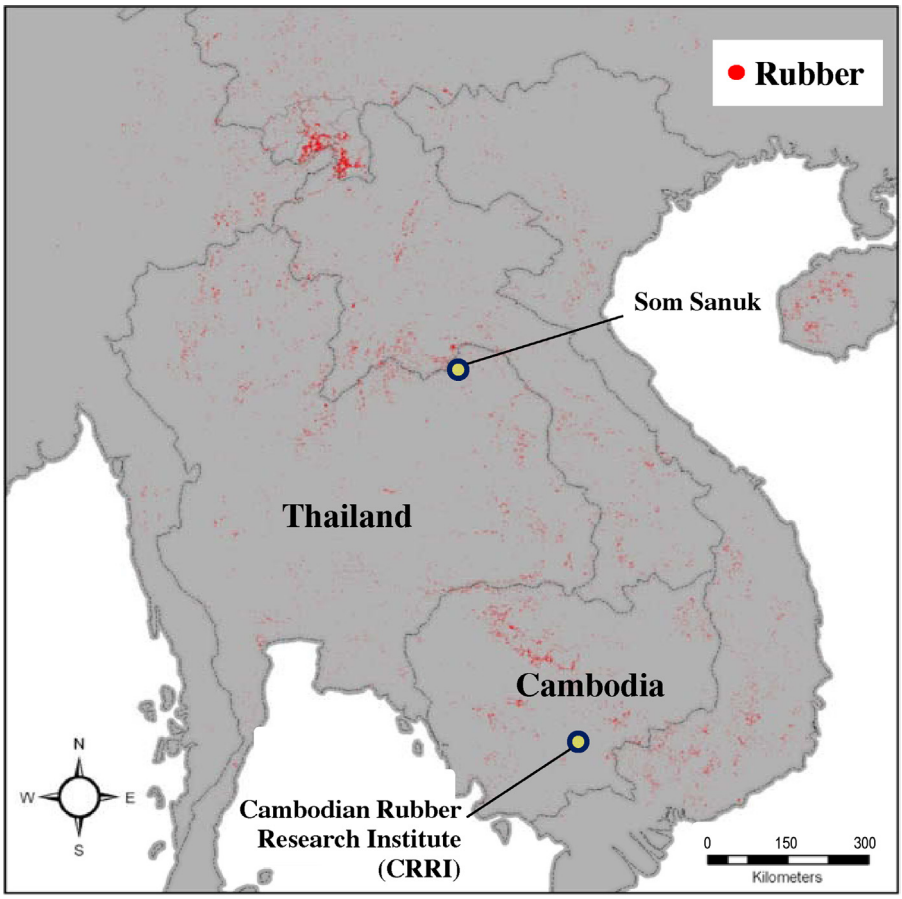

Fig. 1. Locations of rubber plantations in mainland Southeast Asia (red dots) shown along with the study sites: Som Sanuk in northeastern Thailand and Cambodian Rubber Research Institute (CRRI) in central Cambodia. Map is based on Li and Fox (2011). (For interpretation of the references to color in this figure legend, the reader is referred to the web version of this article.)

Hevea rubber originates from the tropical rainforests of the Amazon in South America. Much of the Southeast Asia growing areas are outside the native range, which is intrinsically warm and moist throughout the year (Priyadarshan, 2003, 2005). However, selective breeding of *Hevea* clones has facilitated the expansion of rubber plantations into relatively cool and dry environments, such as those found in montane and monsoonal regions of mainland Southeast Asia. Rubber is now cultivated profitably in many "non-traditional" areas previously determined as unsuitable (Qiu, 2009).

Numerous potential negative ecological and environmental consequences of converting primary and secondary forests into rubber plantations have been suggested: decrease in biodiversity; reduction of total biomass carbon; alteration of the hydrological regime; and acceleration of erosion (Wu et al., 2001; Mann, 2009; Qiu, 2009; Ziegler et al., 2009a,b, 2012; Guardiola-Claramonte et al., 2010; Tan et al., 2011). On the other hand, some studies reported that rubber plantations replacing non-forested lands could act as a carbon sinks (Wauters et al., 2008). Further, while eddy covariance measurements in rubber revealed high plantation water use and a large proportion of energy being used to drive evapotranspiration for most of the year (Tan et al., 2011; Giambelluca et al., submitted for publication, hereinafter referred to as submitted manuscript, 2015), the results of sapflow measurements of individual rubber trees showed water use of rubber plantations may not be as high as anticipated (Isarangkool Na Ayutthaya et al., 2011; Carr, 2012; Kobayashi et al., 2014), but these findings might be related to differences in regional climate, geography, physiological adaptations, and measurement method. Of concern to our research, large-scale land use changes to rubber plantations may have important implications for local-to-regional carbon and water balances, but they still remain unclear. Hindering the ability to predict and understand these changes is lack of information on the characteristics of mass (i.e., CO_2 and H_2O) exchange between rubber plantation canopy and atmosphere, which is the subject of this investigation.

The region encompassing northeastern Thailand and central Cambodia has strong seasonality in precipitation (see Fig. 3 in Kumagai et al. (2005)): well-defined wet and dry seasons are clearly apparent. Although seasonality in atmospheric variables such as air temperature and humidity affect the hydrologic fluxes above and within vegetation, fluctuations in soil moisture and plant water status, influenced by precipitation variations, are the most important controls on the hydrological, atmospheric and ecological processes within the Soil–Plant–Atmosphere Continuum (SPAC) (see Kumagai et al., 2009b). Thus, it is logical to expect that current rubber plantations in northeastern Thailand and central Cambodia must cope with strong seasonal water stress via the SPAC context, such as limiting tree water use by regulating stomatal behavior in response to soil moisture deficit, and compensating for lack of water near the surface during the dry season by exploiting deeper soil water. Further, it is important to note that a previous study (Sangsing et al., 2004) found different rubber clones exhibit varying degrees of adaptability to water stress, thus it would be expected that water use efficiency and risk of hydraulic fracture vary with clone type in a particular climate.

Environmental control of canopy mass exchange and tree water use can be characterized in terms of the relationship between canopy conductance (G_C) and environmental factors. Canopy conductance is thought to result from the bulk leaf stomatal regulations

within the vegetation canopy; and it is generally calculated from the inverted Penman–Monteith equation with measurements of canopy transpiration (e.g., Wullschleger et al., 2000; Delzon et al., 2004; Kumagai et al., 2004, 2008, 2009a; Herbst et al., 2008; Tateishi et al., 2010). Because both CO_2 and H_2O exchanges are regulated by stomata, G_C is a major index of the exchange efficiency and environmental control. However, estimation from above-canopy evapotranspiration (E_T), such as observed using eddy covariance system and above-canopy environmental factors, leads to surface conductance (G_S), not G_C. Briefly, G_C reflects the physiological behavior of the canopy vegetation, while G_S also incorporates the exchange characteristics of the understory vegetation and/or soil surface (see Kelliher et al., 1995).

The present study is built on a previous study that revealed that the rubber E_T, obtained by eddy flux measurements in northeastern Thailand and central Cambodia, is much higher than regional E_T in large-scale estimates in mainland Southeast Asia (Giambelluca et al., submitted for publication). Therefore, our goal is to understand environmental controls on G_C related to the ecosystem water resources in the SPAC context, and how the studied rubber plantations can maintain such high E_T despite existence of strong seasonal water stress. In the present study, we go further and use the eddy fluxes measurements combined with a simple two-layer vegetation evaporation model (e.g., Kelliher et al., 1995) to separate G_C from the G_S. We principally investigate the differences in G_C and the environmental controls between the rubber plantation sites, as well as between rubber and other vegetation. This analysis represents an important step in understanding the impacts of the rapid expansion of rubber plantations on water and carbon cycling in the region.

2. Materials and methods

2.1. Site description

We present an analysis of canopy stomatal behavior of rubber trees at two sites in monsoonal regions of mainland Southeast Asia with contrasting rainfall regimes (Fig. 1): (1) Som Sanuk, Bueng Kan Province, northeast Thailand (18°11′N, 103°25′E, 210 m a.s.l.); and (2) Cambodian Rubber Research Institute (CRRI) in Kampong Cham Province, central Cambodia (11°57′N, 105°34′E, 57 m a.s.l.). For each site, we present the results for two complete years of measurements: February 2009–June 2011 at Som Sanuk; and September 2009–February 2012 at CRRI.

2.1.1. Som Sanuk site

The study site at Som Sanuk is centered within a 2.4-ha smallholder property planted with clone RRIM-600 rubber trees. The average slope of the terrain surrounding the meteorological tower is less than 1°. The A horizon of the soil is very shallow (<10 cm), light gray in color, and has little organic material (<2%). The dull yellow B horizon is 30–70 cm thick, sandy, and is 20–40 cm thicker along tree rows than between rows as a result of the practice of mounding soil along each row before planting. Below the B horizon is a BW horizon, approximately 85-cm thick, with ferralitic concretions. Few roots penetrate the BW horizon, below which is found a gray/brown clay layer. During the two project years (March 2009–February 2010 and March 2010–February 2011), annual precipitation was 2215 and 2020 mm, and mean annual temperature was 26.2 and 26.0 °C, respectively. About 90% of the total annual rainfall occurs during May–September. November– January is relatively cool. Air temperature is generally highest in April. Wind is predominantly from the northeast during October–April, and from the southwest during June through August. The climatic characteristics at Som Sanuk are presented in Fig. 2.

Of the 1360 trees originally planted on the property in 1991, 1260 trees had survived after 20 years. Trees were planted with a spacing of 7.0 m × 2.5 m. The mean canopy height was approximately 19 m and the mean diameter at 1.7 m height was 18.9 cm (standard deviation (SD) = 3.0 cm) in January 2010. During 2010–2012, mean stem diameter growth rate was 0.6 cm $year^{-1}$. Approximately 1.2 kg $tree^{-1}$ of fertilizer (50/50 mix of manure and chemical fertilizers, typically N–P–K: 20–10–12) is applied twice per year. Latex tapping was initiated in about 1997 or 1998. With the exception of a few small riparian areas with shrub vegetation, mature rubber trees form a continuous canopy in all directions for at least 500 m.

2.1.2. Cambodian Rubber Research Institute site

A 6.25-ha plot of clone RRIC-100 in an experimental rubber plantation within the 994-ha Cambodian Rubber Research Institute (CRRI) was used for the observations in central Cambodia (see Kumagai et al., 2013). The experimental rubber plantation is on a level plain set in red basaltic latosols. The soil texture is clay with about 10% fine sand, 10% coarse silt, 20% fine silt and 60% clay. The climatic characteristics at CRRI are presented in Fig. 3. The climate is governed by the Asian Monsoon, which produces two distinct seasons: a wet season (approximately May–October) and a dry season (approximately November–April). Annual precipitation in 2010 and 2011 was 1332 and 1545 mm, respectively. Rainy seasons extended from late-May to late-November in 2010, and late-April to mid-November in 2011. The mean annual temperature was significantly higher in 2010 (28.0 °C) than in 2011 (27.0 °C). For both years, maximum monthly averages occurred in April–May; minimums occurred in December–January.

All the trees at the site were planted in 2004 (i.e., 8 years old in 2012) using a regular spacing of 6-m in north-south direction and 3-m in east–west direction, resulting in a potential tree density of 555 trees ha^{-1}. Due to tree mortality, approximately 20% of trees in mature stands were missing, producing a tree density of 458 trees ha^{-1}. Chemical fertilizer (N–P–K: 15–15–15) was used only during the first 4 years after planting. Latex tapping was initiated in November, 2010. Stem diameters were measured at 1.7 m height above the ground so as not to overlap the tapping panel, which starts at 1.3 m. Mean stem diameter was 13.3 cm (SD = 2.3 cm) in February 2010. This increased to 15.3 cm (SD = 2.3 cm) in March 2012. Mean canopy height was 11.4 m in January 2010, 12.9 m in March 2011, and 14.3 m in March 2012. Various species of herbaceous plants and shrubs occupied the understory; and they fully cover the ground except for along the tappers path.

2.2. Meteorological measurements

Canopy towers 26.5-m and 30-m-tall were constructed at Som Sanuk and CRRI, respectively, for micrometeorological and eddy flux measurements. Air temperature, humidity (HMP45C, Campbell Scientific, Logan, UT), and four-component radiation (at Som Sanuk; CNR1, Kipp & Zonen, Delft, Netherlands, and at CRRI; NR01, Hukseflux, Delft, Netherlands) sensors were installed at the top of each tower. At Som Sanuk, a rain gauge (TE-525, Texas Electronics, Inc., Dallas, TX) was mounted at a height of 20 m on the southwest side of the tower. At CRRI, two rain gauges (TE-525) were mounted at a height of 15 m on the southwest and northeast sides of the tower. To minimize bias from tower interference and wind-related measurement error, rain gauges were mounted close to the canopy top. At CRRI, rainfall from the upwind gauge was used based on the mean wind direction observed in each 30-min interval. Samples were taken at 10 Hz for radiation, air temperature, and humidity and averaged over 30 min. Precipitation (P) was measured by counting tipping bucket tips (CR3000 and CR23X, Campbell Scientific) at an interval of 30-min.

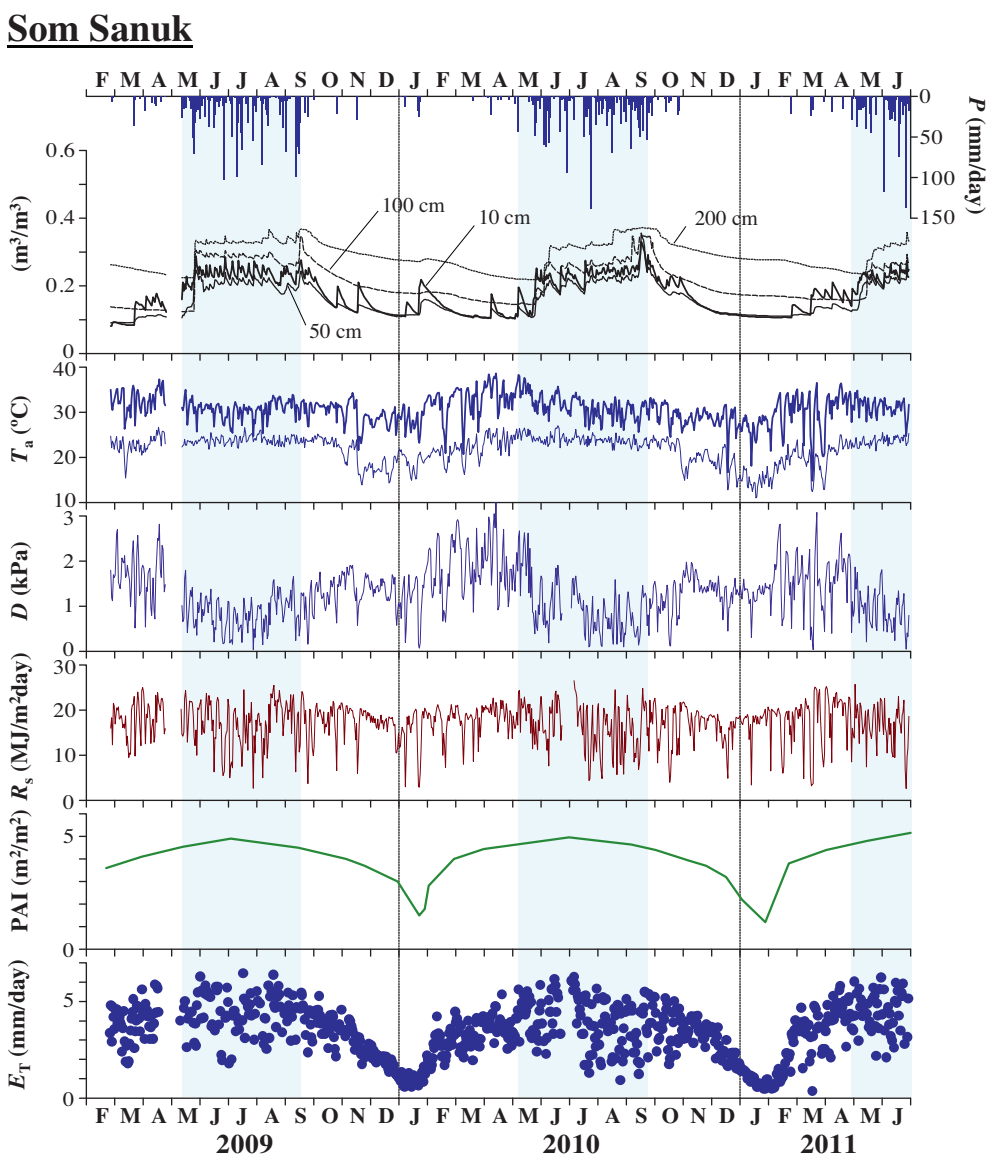

Fig. 2. Climatic data at Som Sanuk in Thailand: (from the top): daily precipitation (P; bars); volumetric soil moisture content at each depth (θ; lines); daily maximum (thick line) and minimum air temperature (T_a); mean daytime vapor pressure deficit (D); daily total solar radiation (R_s); plant area index (PAI); and daily total evapotranspiration from a whole ecosystem (E_T). Shaded columns represent periods of wet season.

Photosynthetic photon flux density (PPFD) below the canopy was measured below the canopy at a height of approximately 3.0 m at Som Sanuk with line quantum sensors (SQ-311, Apogee Instruments, Logan, UT). At CRRI, intensive observations on the transmitted PPFD through the canopy were conducted at approximately 1-m above the forest floor by walking along 53.6-m and 60.3-m straight transects with a quantum sensor (MIJ-14PAR, Environmental Measurement Japan Co. Ltd., Fukuoka, Japan) mounted at one end of supporting arm (see Kumagai et al., 2013). The data on PPFD below the canopy at Som Sanuk and CRRI were used for estimating radiative energy absorbed within the rubber tree canopy and determining the relationship between the absorbed radiative energy and the amount of foliage for each site.

Volumetric soil water content (θ) was measured through a depth profile at each site using time domain reflectometers (TDR; CS616, Campbell Scientific). TDRs were placed at depths (orientations) of 0.04 m (horizontal), 0.04–0.34 m (vertical), 0.48–0.75 m (vertical), 0.80 m (horizontal), 1.50–1.80 m (vertical), and 2.20–2.50 m (vertical) at Som Sanuk, and at 0.04 m (horizontal), 0.35–0.65 m (vertical), 1.05–1.35 m (vertical), 2.03–2.33 m (vertical), and 3.08–3.38 m (vertical) at CRRI. At each site, soil heat flux (G) was estimated from measurements taken at a depth of 8 cm with four soil heat flux plates (HFP01, Hukseflux) and the calculated change in soil heat storage in the upper 8 cm layer based on soil temperature and soil moisture measurements. The data were recorded with a data logger (CR23X) at 30-min intervals.

2.3. Eddy covariance measurements

The latent heat flux (LE_T, where L is the latent heat of vaporization of water) and sensible heat flux (H) were measured using the eddy covariance technique. At each site, a three-dimensional sonic anemometer (CSAT3, Campbell Scientific) and an open-path CO_2/H_2O analyzer (LI-7500, Li-Cor, Lincoln, NE) were installed (at 26.5 and 30.1 m height, at Som Sanuk and CRRI, respectively). The CSAT3 and LI-7500 sensor orientations were switched seasonally toward the southwest in wet season, and the north in dry season (the seasonal predominant wind directions). Reorienting the sensors was necessary to minimize effects of turbulence from the tower structure on the eddy covariance measurements.

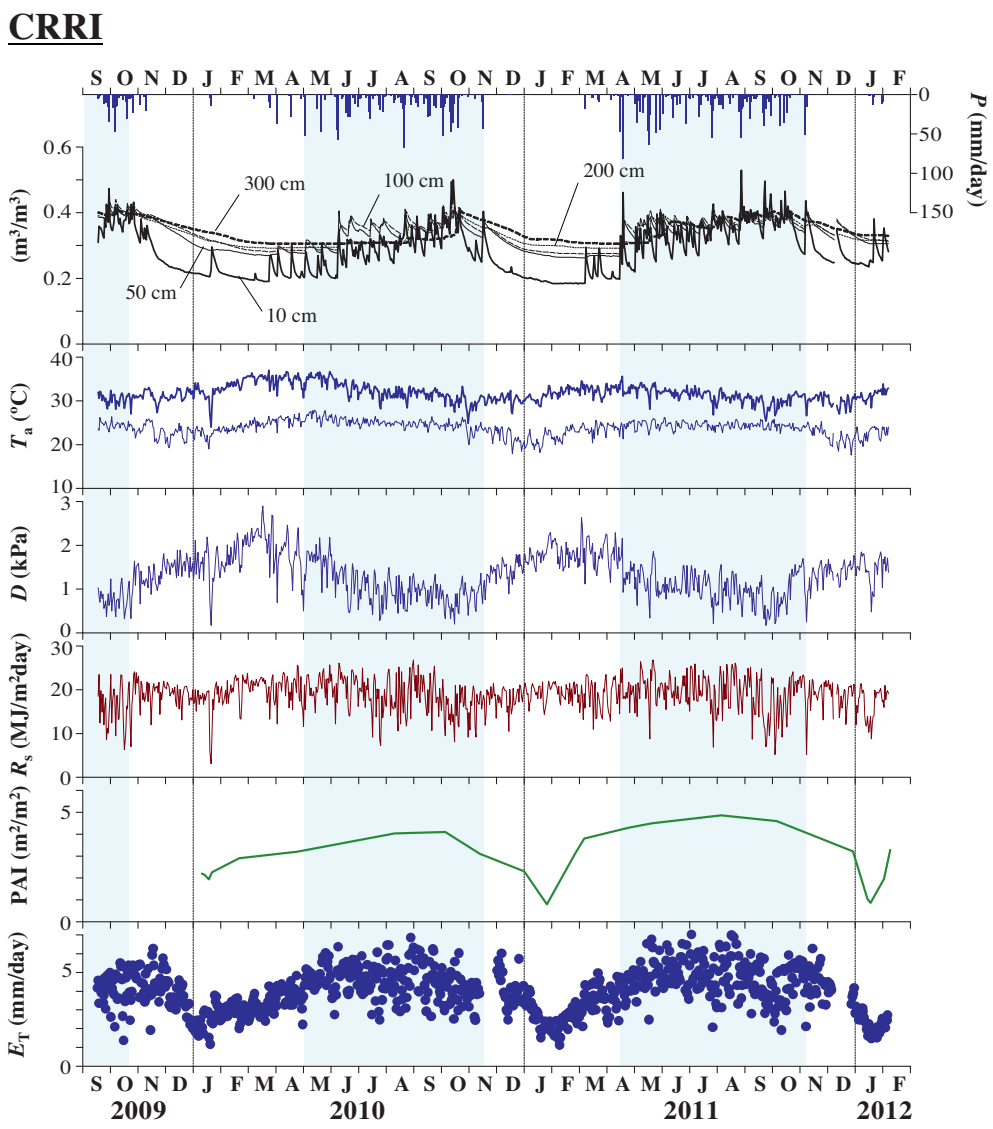

Fig. 3. Climatic data at Cambodian Rubber Research Institute (CRRI) in Cambodia: (from the top): daily precipitation (P; bars); volumetric soil moisture content at each depth (θ; lines); daily maximum (thick line) and minimum air temperature (T_a); mean daytime vapor pressure deficit (D); daily total solar radiation (R_s); plant area index (PAI); and daily total evapotranspiration from a whole ecosystem (E_T). Shaded columns represent periods of wet season.

Wind speeds and gas concentration time series were all sampled and stored at 10 Hz on a datalogger (CR3000). All variances and covariances required for the eddy covariance flux estimates were computed over a 30-min averaging interval. The details of screening, filtering, and post-processing of 10 Hz data to compute 30-min fluxes are given by Giambelluca et al. (submitted for publication).

The ratio of mean annual $LE_T + H$ to mean annual available energy (A), which was estimated as net radiation minus G and heat storages in within-canopy air and above-ground biomass, was 0.94 for Som Sanuk and 0.88 for CRRI. Here, we employed a "moving window energy closure ratio $(LE_T + H)/A$" method for closing the canopy surface energy balance for each 30-min interval. LE_T data gaps were filled with values estimated from the relationship between actual LE_T and A. The details of energy closure adjustment and gap filling are also given by Giambelluca et al. (submitted for publication).

In this study, we identified and removed 30-min averaged eddy fluxes during which rainfall occurred. This was done because our main objective is to investigate environmental control of G_C, derived from dry canopy E_T. Importantly, the open-path analyzer was mounted in an inclined orientation and the values of AGC (Automatic Gain Control) were used to eliminate abnormal flux values, so as to reduce problems of rain and dew droplets sitting on the window. Despite high annual precipitation at these sites, rainfall during the wet season frequently occurs in short bursts, thus wet sensor interruptions are relatively minor compared to sites with similar rainfall totals that are more frequently wet.

2.4. Leaf area index measurements

The silhouette area index of leaves plus stems and branches (plant area index; PAI) was measured using a pair of plant canopy analyzers (PCA) (LAI-2000 or LAI-2200, Li-Cor) at irregular time intervals over the course of the study at an interval of 6 and 5 m at Som Sanuk and CRRI, respectively, along transects oriented diagonally with respect to tree rows. The PAI measurements were conducted frequently during leaf shedding and flushing periods in 2010 and 2012, and periodically throughout other years to approximate the annual cycle of foliage accumulation and loss throughout

the study period. While optical PCA measurements are limited, estimation of the seasonal pattern of PAI is based on the best available data at the sites, and the analysis to estimate the pattern of the annual cycle in each year is independent of the flux data. Because the measurements in 2011 were scarce or unavailable, seasonal variation was estimated based on the measured value near the time of maximum PAI in August 2011 and on the annual cycles of 2010 and 2012, and 2013, years which had more frequent PCA observations. Bi-weekly litterfall collections were also used to verify the patterns of leaf loss during the leaf shedding period. Additionally, the timing of leaf fall and leaf area recovery were estimated based on albedo measurements and visual observations.

Kucharik et al. (1998) and Bréda (2003) suggested that PAI detected by PCA denotes leaf area index (LAI) in the period when the foliage can mask the woody area, but stems cannot be overlooked in the leaf-fall period. Also, Pokorný and Marek (2000) confirmed that a common use of the LAI-2000 tends to underestimate LAI because the large zenith angle readings include the effect of woody areas, especially, stems. Therefore, PCA measurements were adjusted by masking the ring at the lowest angle (centered at 68° zenith angle) which can only see stems. Masking consecutive lower angles in mature rubber plantations caused a consistent increase in calculated LAI with PCA. The studied rubber canopies at both Som Sanuk and CRRI were completely dormant (i.e., LAI = 0) on the day of the lowest PAI, but the period for such dormant days is less than one month (see Figs. 2 and 3). Therefore, we could assume that for both Som Sanuk and CRRI, the time course of LAI was equal to that of PAI, except for January, when LAI was calculated by subtracting the minimum PAI during the studied period from the yearly PAI. At both sites, January is the leaf-fall period, and thus, was not used for the examination of the environmental stomatal control (described later).

2.5. Calculation of soil water balance

Because slopes at both Som Sanuk and CRRI are gentle, lateral soil water movement can be neglected. Vertically integrated soil water balance equation is then given by:

$$\int_{t_1}^{t_2} [P(t) - E_T(t)]\,dt - \int_0^z \left[\theta(z,t_2) - \theta(z,t_1)\right] dz = 0 \quad (1)$$

where t is time, t_1 and t_2 are temporal points in the time course, and z is soil depth. It should be noted that leakage at z is neglected in Eq. (1). The first term in the right-hand side of Eq. (1) was referred to as actual water balance, $P - E_T$. The second term denotes the difference between soil water content at t_2 and t_1 (Δw). $\int_0^z \theta dz$ in the second term was computed as follows: (1) estimating θ_{10}, θ_{50}, θ_{100}, θ_{200}, and θ_{300} (where each subscript denotes the soil depth (in cm) for each θ) by weighted-averaging the measured θ profiles (see Figs. 2 and 3); and (2) integrating θ along z such as $300\theta_{10} + 450\theta_{50} + 750\theta_{100} + 500\theta_{200}$ and $300\theta_{10} + 450\theta_{50} + 750\theta_{100} + 1000\theta_{200} + 500\theta_{300}$ (in mm) for the 0–2 m (at Som Sanuk) and the 0–3 m (at CRRI) soil layers, respectively.

Potential evaporation (E_{T_POT}) was an expression represented by Priestley and Taylor (1972):

$$E_{T\_}POT = \alpha_{PT} \frac{\Delta A}{L(\Delta + \gamma)} \quad (2)$$

where α_{PT} is the Priestley–Taylor coefficient (=1.26), Δ is the rate of change of saturation water vapor pressure with temperature, A is the total available energy ($R_n - G$; where R_n is net radiation), and γ is the psychometric constant. $\int_{t_1}^{t_2} [P(t) - E_{T\_POT}(t)]\,dt$ was referred to as potential water balance, $P - E_{T\_POT}$.

2.6. Calculation of canopy stomatal conductance

The surface conductance (G_s), representing the efficiency of exchange between the top of the vegetation surface and the atmosphere, was calculated by applying the actual data of LE_T to the inverted Penman–Monteith equation as:

$$G_s = \frac{G_a \gamma LE_T}{\Delta A_c + \rho C_p G_a D - (\Delta + \gamma) LE_T}, \quad (3)$$

where ρ is the density of dry air, C_p is the specific heat of air at a constant pressure, and D is the vapor pressure deficit above the canopy. Aerodynamic conductance, G_a, was estimated as u^{*2}/u, where u^* is the friction velocity and u is wind speed above the canopy.

Canopy conductance (G_c), representing the efficiency of the canopy transpiration (LE_c), was calculated according to Kelliher et al. (1995) with some modifications:

$$G_c = \frac{G_a \gamma LE_c}{\Delta A_c + \rho C_p G_a D - (\Delta + \gamma) LE_c}, \quad (4)$$

for which

$$A_c = A - A_s \quad (5)$$

$$A_s = A \exp\left(-\alpha PAI^b\right) \quad (6)$$

In Eqs. (5) and (6), A_c and A_s are the total available energy absorbed by leaves within the canopy and at the vegetation floor, respectively; and a and b are the extinction coefficient and fitting parameter, respectively. The parameters a and b were estimated using nonlinear least squares regression between values of A_s calculated from Eq. (6) and obtained by the radiation observations above and below the canopy. On the basis of our regression analysis, we obtained values of $a = 0.34$ and $b = 1.47$ for both Som Sanuk and CRRI. LE_c can be expressed as a contribution from the canopy to the total vegetation latent heat flux:

$$LE_c = LE_T - LE_s, \quad (7)$$

for which

$$LE_s = \alpha_s \frac{\Delta A_s}{\Delta + \gamma}, \quad (8)$$

where LE_s is latent heat flux at the vegetation floor, and α_s is an empirical parameter representing evaporative efficiency. The parameter α_s was estimated to be 0.3 and 0.5 for Som Sanuk and CRRI, respectively, under the leaf-less (i.e., LAI = 0) conditions, where LE_T can be assumed to be equal to LE_s. Also, we assumed that the α_s determined in the dry season might not cause large error in estimating LE_s during the wet season because of relatively small values of A_s in the leafy and wet season.

We assumed that G_c is the parallel sum of the individual leaf stomatal conductances (e.g., Raupach and Finnigan, 1988), giving:

$$g_s = \frac{G_c}{LAI} \quad (9)$$

where g_s is mean canopy stomatal conductance per unit leaf area ($m\,s^{-1}$, canopy stomatal conductance: see Pataki and Oren, 2003). Note that for the quality control, we removed the g_s values obtained when $D \leq 0.6$ kPa (Ewers and Oren, 2000).

2.7. Stomatal conductance model

To facilitate the interpretation of the influence of environmental variables on stomatal behavior, a multiplicative-type function is commonly used with determining parameters contained in each function by appropriate nonlinear regression analysis (see Jarvis,

1976). Oren et al. (1999) focused on the relationship between stomatal conductance and D as follows (see Kumagai, 2011):

$$g_s = g_{sref} - m \ln D \quad (10)$$

where g_{sref} is the reference value of g_s (i.e., the value of g_s at $D = 1$ kPa) and m is the sensitivity of g_s to D (i.e., $-dg_s/d\ln D$). The model of Oren et al. (1999), i.e., Eq. (10), has been developed to analyze a leaf-level stomatal (g_s) response to atmospheric evaporative demand (D) employing the mean canopy stomatal conductance derived from individual tree canopy conductance, which is estimated by the sapflow measurement, divided by total leaf area for an individual tree (see Pataki and Oren, 2003). In other words, the stomatal characteristics such as the parameters g_{sref} and m are usually estimated for individual trees. In this study, we used ecosystem-level evapotranspiration (E_T) observed by eddy covariance measurements. Separating dry-canopy evaporation, i.e., canopy transpiration (E_c), from E_T and individual tree level stomatal behavior derived from canopy level one because of the even-sized trees within each study site enabled us to compare the Oren et al. model parameters obtained in the study sites and other studies.

A boundary line analysis on the relationships between D and g_s can be used for determining the parameters g_{sref} and m (e.g., Schäer et al., 2000; Ewers et al., 2001, 2005). The boundary line was derived by regressing Eq. (10) with data obtained as follows: (1) selecting g_s when solar radiation, R_s, ≥ 600 W m^{-2}; (2) partitioning the g_s response to D into 0.5 kPa D intervals; (3) removing outliers within each interval of D ($p < 0.05$ Smirnov–Grubbs test); and (4) selecting data above the mean plus one standard deviation of g_s and averaging the selected data for each D interval. Midday data (1000–1400 LT) were used for the analyses examining the environmental control of g_s. The maximum contributions to rainfall were in the mid-night and early morning at Som Sanuk and in the mid-night at CRRI. In addition, the data were selected on the condition of high R_s, under which the open-path sensor window is likely to dry out quickly after the morning rainfall. The qualified data at Som Sanuk was 76.8% and 79.8% at CRRI, a high ratio considering the high annual rainfall at these sites.

3. Results

3.1. Environmental and eddy flux data

For both sites, there was little seasonality in the mean daily R_s (Figs. 2 and 3): a decrease in R_s caused by cloud cover in the wet season was compensated by the higher solar elevation during the wet season (see Kumagai et al., 2009b). The seasonal variation in solar elevation along with the annual moisture cycle produces cool (November to mid-February) and hot dry (March–May) seasons. The additional effect of cloud cover in the wet season results in sinusoidal variations in T_a: annual maximum and minimum T_a appear in hot and cool dry seasons, respectively, for both sites (Figs. 2 and 3). Therefore, for both sites, D also shows a seasonal and sinusoidal variation, but unlike T_a, minimum D appears in the wet season; and the maximum in hot dry season (Figs. 2 and 3).

Wang and LinHo (2002) developed a universal way to define the onset and withdrawal dates of the wet season over the entire Asian summer monsoon region. According to their result using the global climatological 5-day mean rainfall dataset for the 20-year period (1979–1998), the onset and withdrawal dates (DOY) were 135 and 275, respectively, at Som Sanuk, and 155 and 295, respectively, at CRRI. This suggested that on the normal conditions, onset and withdrawal of the wet season are prone to be 20 days earlier at Som Sanuk than at CRRI, although the wet season length for the two sites are the same (ca. 140 days).

Here, we applied Wang and LinHo's (2002) criteria with January mean precipitation for 2010–2011 at Som Sanuk and 2010–2012 at CRRI for each studied year (Figs. 2 and 3). As a result, at Som Sanuk, the onset and withdrawal dates (DOY) were 131 and 256, respectively, in 2009, when the onset came earlier and the period of wet season became shorter than for normal years. There, in 2010, the onset and withdrawal dates were 126 and 266, respectively, coming earlier than for normal years, but the length of wet season was the same as a normal year. In comparison, at CRRI, the onset and withdrawal dates were 121 and 316, respectively, in 2010, and 101 and 305, respectively, in 2011. There, for both studied years, the onset and withdrawal were much earlier and later than for normal years, inducing much longer wet season (ca. 200 days).

For both sites, the periods of full-leaf-fall were, at most, around one month (Figs. 2 and 3). This also means that rubber trees are leafy even during most parts of dry season. Annual rate of P was 2118 mm, compared with E_T estimate of 1128 mm at Som Sanuk. These values at CRRI were 1439 and 1272 mm, respectively (see Figs. 2 and 3; Giambelluca et al., submitted for publication). After adjustment for energy closure, the annual E_T became 1221 mm for Som Sanuk and 1459 mm for CRRI (Giambelluca et al., submitted for publication). Thus, two major questions arise: (1) what factors sustain such high E_T of rubber plantations, especially at CRRI, where the annual P and E_T were similar; and (2) what factors sustain the persistence of the E_T during the dry season, especially during the late (hot) part of the dry season, when the ecosystem water resources must be limited.

3.2. Tree water use and soil water balance

E_{T_POT}, E_T, and P for each site are compared for each season (i.e., December–February: DJF, March–May: MAM, June–August: JJA, and September–November: SON) in Fig. 4. Negative values of potential water balance ($P - E_{T\_POT}$) indicate seasons when the ecosystem experienced water resource deficits, i.e., in DJF and MAM 2010 and DJF and MAM 2011 at Som Sanuk and in MAM 2010, DJF and SON 2011, and DJF 2012 at CRRI (Fig. 4). Actual water balance ($P - E_T$) was almost zero, indicating that tree water use regulation might be a major controlling factor in MAM of 2011 at Som Sanuk and in SON of 2011 at CRRI.

We found that in the season when $P - E_T$ was negative (DJF and MAM 2010 and DJF 2011 at Som Sanuk, and MAM 2010, DJF 2011 and 2012 at CRRI), the $P - E_T$ was compensated with residual soil water stored during the previous season (Δw) in the 0–2 m soil layer at Som Sanuk and 0–3 m soil layer at CRRI (Fig. 4). Here, we should note that the Δw might reflect the $P - E_T$ plus leakage from the bottom of soil layer and, therefore, represents the maximum limit of the actual compensation for the $P - E_T$. Such compensation for the tree water use deficit might have been achieved by a combination of utilization of the carry-over soil water and the tree water use regulation.

3.3. Tree water use regulation via stomatal behavior

Seasonal patterns of midday (1000–1400 LT) averaged G_s, G_c and g_s, as major indices for depicting the tree water regulation, are compared at both sites in Fig. 5. In the entire studied period, the G_s reached as high as 25 mm s^{-1} at Som Sanuk and 30 mm s^{-1} at CRRI in the wet seasons; and the minimum value was about 2 mm s^{-1} at both sites in the dry seasons (Fig. 5a and c). On the other hand, maximum and minimum values of the G_c were approximately 25 mm s^{-1} at Som Sanuk and 30 mm s^{-1} at CRRI in the wet seasons; and they were almost zero at both sites in the dry season when trees were leaf-less (Fig. 5a and c). The differences between G_s and G_c, due to the contribution of understory and soil (floor) evapotranspiration (E_{T_fl}) to the total E_T, were somewhat constant (at

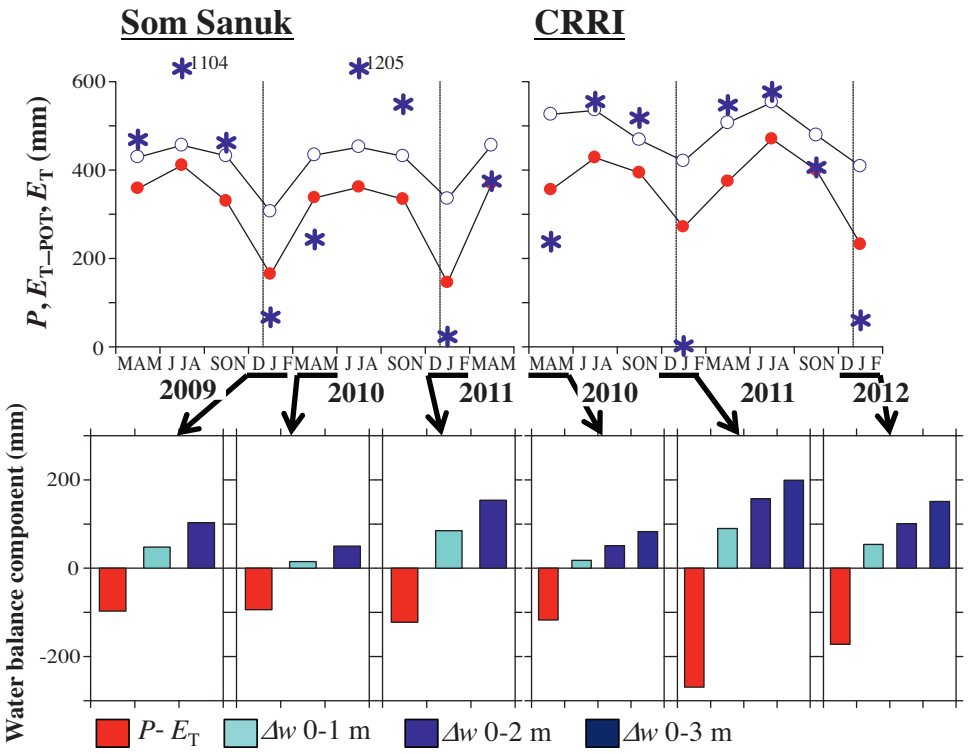

Fig. 4. Upper panel: precipitation (P; asterisks), whole ecosystem evapotranspiration (E_T; closed circles), and potential evaporation (E_{T_POT}; open circles) for each season (i.e., December–February: DJF; March–May: MAM; June–August: JJA; and September–November: SON) at Som Sanuk and Cambodian Rubber Research Institute (CRRI). Lower panel: actual water balance ($P - E_T$) and residual soil water stored during the previous season (Δw: difference between mean soil water at a given season and the previous season) in 0–1, 0–2 and 0–3 m soil layers in the season of $P - E_T < 0$.

most 2 mm s^{-1}), and thus, the E_{T_fl} was not thought to vary appreciably throughout the studied period. It is reasonable to assume E_{T_fl} to be invariant, given that some partial cancelations emerge –for example lower radiative energy reaching the understory and soil in the leafy and wet season is likely to result in the lower E_{T_fl}; however, low soil moisture in the leaf-less and dry season also induces lower E_{T_fl}. Although g_s was estimated as G_c divided by LAI (see Eq. (9)), the seasonal variation in the g_s was similar to the variation in G_c in that the g_s gradually increased with leaf-out and leaf-expansion, and decreased with leaf-fall (Fig. 5b and d, see

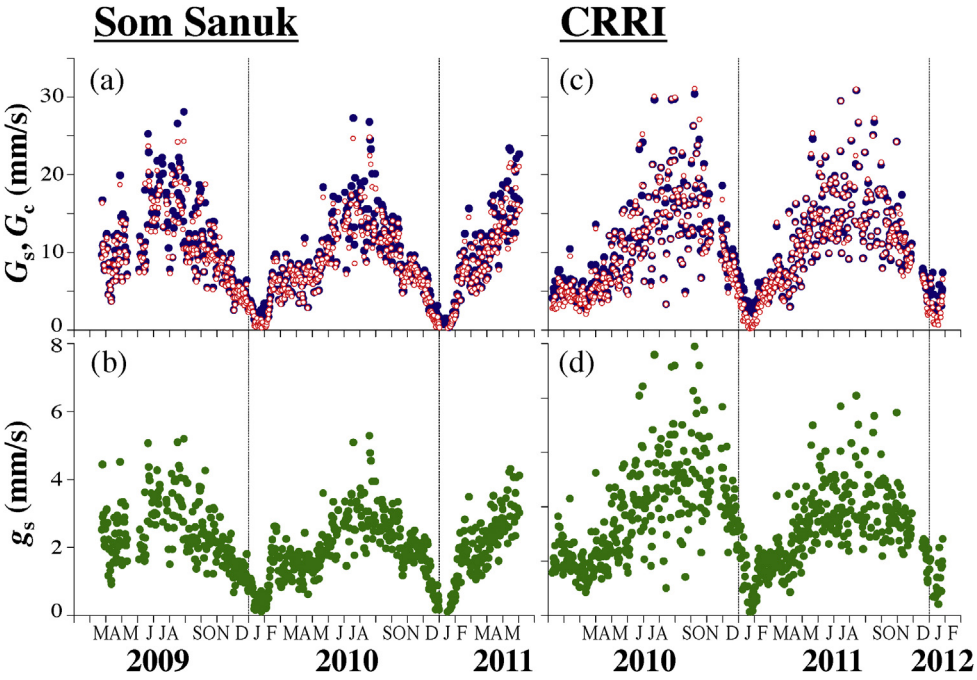

Fig. 5. Panels a and c: seasonal patterns of midday (1000–1400 LT) averaged surface conductance (G_s; closed circles) and canopy conductance (G_c; open circles) at Som Sanuk, Thailand and the Cambodian Rubber Research Institute (CRRI), Cambodia. Panels b and d: canopy stomatal conductance (g_s) at Som Sanuk (b) and CRRI (d).

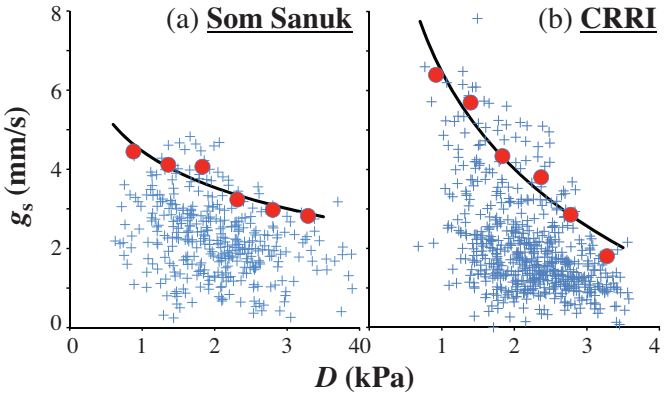

Fig. 6. Representative relationships between vapor pressure deficit (D) and canopy stomatal conductance (g_s: pluses) on a 30-min basis (1000–1400 LT) in March–May (MAM), 2009 at (a) Som Sanuk and in MAM 2010 at (b) Cambodian Rubber Research Institute (CRRI). Circles represent the data selected by the boundary line analysis (see text; Section 2.7), to which Eq. (10) was fit (lines).

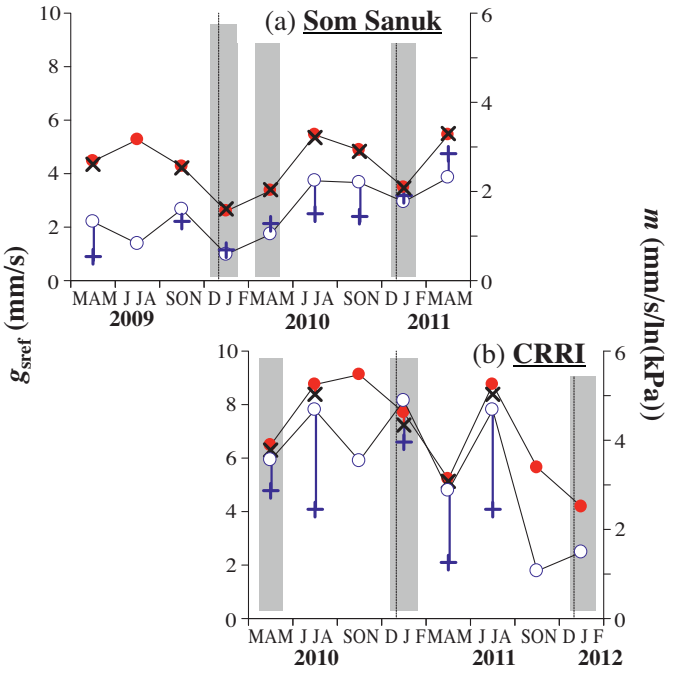

Fig. 7. Seasonal variations in canopy stomatal conductance (g_s) at vapor pressure deficit (D) = 1 kPa (g_{sref}; closed circles) and sensitivity of g_s to D (m) (=$-dg_s/d\ln D$): (open circles) at (a) Som Sanuk and (b) Cambodian Rubber Research Institute (CRRI). Values of g_{sref} (crosses) and m (pluses) estimated with a narrower range of D (upper limit: 2 kPa) are also shown. December–February: DJF, March–May: MAM, June–August: JJA, and September–November: SON. Note that the narrower D range estimations for g_{sref} and m were not made in JJA, 2009 at Som Sanuk and in SON, 2010, SON, 2011 and DJF, 2011–2012 at CRRI because of their original narrow range of D. Shaded columns represent periods when actual water balance ($P - E_T$) was negative (see Fig. 4).

also Figs. 2 and 3). The gradual increase in gs after leaf expansion might be due to a maturation process in the photosynthetic capacity of leaves (see Wilson et al., 2001). Interestingly, the g_s decreased after August at Som Sanuk and after September–October at CRRI, corresponding to an earlier withdrawal of wet season at Som Sanuk (in September) than at CRRI (in November). This steep decrease in the g_s also might be due to change in the leaf-scale physiological status, i.e., leaf-senescence.

3.4. Analyses of stomatal conductance

The representative relationship between D and g_s in MAM at both sites (Fig. 6) shows a general tendency of g_s to decline with increasing D. We obtained the reference conductance, g_{sref}, and the rate of decline in g_s, m, by fitting Eq. (10) to the upper boundaries of the D–g_s data. The MAM analysis period encompasses the end of the dry season and start of the wet season, i.e., the onset of a wet season was in mid-May at Som Sanuk (see Fig. 6a) and early May at CRRI (see Fig. 6b). Thus, although there was not a significant difference in hydro-climate conditions between Som Sanuk and CRRI, g_{sref} and m were significantly higher at CRRI than at Som Sanuk.

Fig. 7 compares seasonal variations in g_{sref} and m at Som Sanuk and CRRI. As ranges of D in the D–g_s plots (see Fig. 6) are critical for the estimations of g_{sref} and m (e.g., Herbst et al., 2008; Schmidt-Walter et al., 2014), we further estimated g_{sref} and m with a narrower range of D (upper limit: 2 kPa) (Fig. 7). In the common study year 2010, even if taking into consideration the lowered values by the narrower D range estimations, both g_{sref} and m were larger at CRRI than at Som Sanuk. The g_{sref} values were robust regardless of the range of D values, while m values were appreciably altered, in particular, much for CRRI, by the narrower range estimations. At Som Sanuk, g_{sref} reached a minimum when $P - E_T < 0$; and the variation in m is similar to that for g_{sref} (Fig. 7a). On the other hand, at CRRI, minimum g_{sref} did not coincide with a condition of $P - E_T < 0$; minimum g_{sref} appeared in MAM, 2011, which, despite being mostly within the dry season, had a positive water balance ($P - E_T > 0$, Fig. 7b). At CRRI, g_{sref} and m was lower from SON and DJF in 2011–2012 as compared to the same seasons in 2010–2011 (Fig. 7b), probably because the wet season withdrawal was earlier in 2011 than in 2010 and other normal year (see Fig. 4), and it may also be explained by differences in leaf emerging and senescence patterns between 2010 and 2011 as the stand matured, as lower leaves remained on the trees until the end of the dry season in 2010, and a secondary flushing of lower leaves emerged in mid-2010. The CRRI g_s started decreasing in mid-October in 2011, however not until early December in 2010 (see Fig. 5). Note that it was confirmed that difference in LAI estimates between SON 2010 (about 4.0) and 2011 (about 4.5) did not significantly alter the decreasing trend in the g_s in 2011.

The 0.6 proportionality (m/g_{sref}) results from the regulation of the minimum leaf water potential (ψ_L) to prevent excessive xylem cavitation, while a value less than 0.6 denotes less strict regulation of ψ_L (Oren et al., 1999; Ewers et al., 2005, 2007). We showed seasonal variations in the m/g_{sref} ratio estimated by both the conventional and the narrower D range methods with the 0.6 proportionality at Som Sanuk and CRRI in Fig. 8. Rubber trees at Som Sanuk had a proportionality significantly lower than 0.6, with only one point greater than 0.5 (for all points: m/g_{sref} = 0.16–0.51: cf., the proportionality 0.51 appeared when $P - E_T < 0$), implying these trees allow the minimum ψ_L to drop with increasing D. While for CRRI, five of eight points were close to the 0.6 proportionality line (for all points: m/g_{sref} = 0.19–0.64), showing somewhat strict stomatal regulation of the minimum ψ_L. The CRRI proportionalities that were much less than 0.6 (Fig. 8) were apparently due to much lower g_{sref} and m from mid-2011–2012 (see Fig. 7b). Here, we have to note that the theoretical proportionality decreases from 0.68 to 0.53 as the D range broadens from 1 to 3 to 1–5 kPa (Oren et al., 1999), implying that the 0.6 proportionality might be valid only for a D range of 1-4 kPa. Thus, we recognize that although estimating the proportionality using the narrower D range would contain some additional uncertainty in the data interpretation, the evidence suggests a tendency for rubber trees at CRRI to regulate their stomatal behavior more strictly than those at Som Sanuk when $P - E_T < 0$ (Fig. 8).

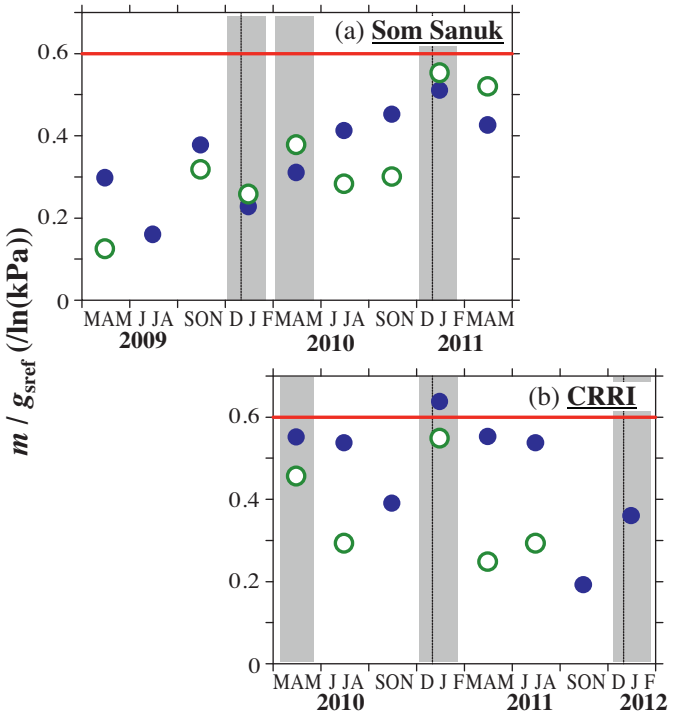

Fig. 8. Seasonal variations in ratio of m (sensitivity of canopy stomatal conductance (g_s) to vapor pressure deficit (D); $-dg_s/d\ln D$) to g_{sref} (g_s at D = 1 kPa) (m/g_{sref}: closed circles) at (a) Som Sanuk and (b) Cambodian Rubber Research Institute (CRRI). Values of m/g_{sref} estimated with a narrower range of D (upper limit: 2 kPa) are also shown (open circles). Note that the narrower D range estimations for g_{sref} and m were not made in JJA, 2009 at Som Sanuk and in SON, 2010, SON, 2011 and DJF, 2011–2012 at CRRI because of their original narrow range of D. The theoretical ratio 0.60 (Oren et al., 1999) is shown by a solid line for each site.

4. Discussion

Guardiola-Claramonte et al. (2008) surmised that the introduction of rubber plantations may reduce stream flow leading to drier conditions throughout a catchment area, mainly because of high water use by rubber trees at the very peak of the dry season (cf., Fox et al., 2014). As rubber trees originate from the Amazonian basin where it is rainy for most of the year, they are intrinsically adapted to moist environments (Priyadarshan et al., 2005). In mainland of Southeast Asia, however, a dry season extends from approximately November–April, during which rubber trees shed their leaves over a short period of time (Figs. 2 and 3). They then initiate leaf-out by the beginning of February, well before the onset of wet season. Rubber trees in this region appear to remain physiologically active for producing new leaves and buds during the dry season by depleting soil water from deep within the soil (see Fox et al., 2014).

Following on previous work, our main concern is to confirm that rubber plantations act as "water pumps" (see Tan et al., 2011) and to determine how they consume such a large volume of water despite the long dry season in this region. Using multi-year E_T flux observations, our prior work revealed that rubber E_T is higher than that of other tree-dominated land covers in mainland Southeast Asia (Giambelluca et al., submitted for publication). Herein, we examined how the rubber trees used the ecosystem water resources, especially in the dry season, and then, how environmental and biological factors affect their canopy stomatal behavior under both water stress and non-stress conditions. We used a combination of the E_T flux data and an inverted version of a simple 2-layer E_T model to estimate stomatal regulation of tree water use, that is, g_s. This analysis enabled us to extract the rubber canopy conductance from total surface conductance, including the canopy and the understory and soil effects. As a result, we demonstrated how each studied rubber plantation copes with strong seasonal drought in terms of tree water use strategy.

Potential water balance ($P - E_{T\_POT}$) for each season can represent the need for tree water use control, mainly by stomatal regulations, and needs for accessing previously stored soil water (Fig. 4). Rubber trees in the season when actual water balance ($P - E_T$) was negative rely on carried-over soil water from the previous season. Investigation of the temporal variation in soil moisture profiles revealed that such negative $P - E_T$ was compensated with soil water carried over from the previous season in the 0–2 m soil layer in Som Sanuk and the 0-3 m soil layer in CRRI. Many studies have reported that majority of tropical trees can avoid severe water stress via deep soil water utilization during the dry periods (e.g., Nepstad et al., 1994; Markewitz et al., 2010; Stahl et al., 2013). On the other hand, according to a global analysis of main root distributions (Jackson et al., 1996), 97% of main roots in tropical deciduous forests are, on average, in the top 1 m. In reality, empirical knowledge for rubber plantation management in CRRI suggested that the rubber tree main-rooting depth should reach at most down to 1 m. Notwithstanding such insufficient rooting depth, soil moisture profiles and visual observations of some deep fine roots showed the studied rubber trees evidently extracted water from 2 and 3 m deep in the soil. Stahl et al. (2013) pointed out that the vertical distribution of root biomass does not perfectly reflect the depth of tree water uptake, and thus we need further investigation about the ability of the fine root system to explore the deeper soil layers.

At both sites, g_s started to decrease earlier than the initiation of leaf-fall and withdrawal of the wet season (see Figs. 2, 3 and 5). Interestingly, despite almost the same timing for leaf-fall at Som Sanuk and CRRI, the g_s started to decrease about one month earlier at Som Sanuk than at CRRI. This might be because the wet season withdrawal occurs more than one month earlier at Som Sanuk than at CRRI, as inferred from our observations and those of Wang and LinHo (2002). Also, at both sites, the intrinsic capacity of g_s appeared to start to recover immediately after the initiation of leaf-out, and the value of g_s gradually increased as the wet season proceeded (see Figs. 2, 3 and 5). These trends implied that the increases and decreases in the g_s were induced by not only environmental perturbation but also temporal variation in intrinsic leaf physiological traits such as photosynthetic capacity (see Kitajima et al., 2002).

There are promising indices for examination of the environmental and biological control of stomatal behavior, i.e., the reference value of g_s (g_{sref}) and the sensitivity of g_s to D (m) (Oren et al., 1999). Among these parameters, g_{sref} is thought to represent intrinsic and maximal capacity of g_s. Compared with the reported values of g_{sref}, collected from various biomes (Oren et al., 1999), maximum g_{sref} observed in this study (estimated to be 360 mmol m^{-2} s^{-1}) was in their upper range; and even the minimum value (≈150 mmol m^{-2} s^{-1}), which appeared in the mid dry season, was somewhat common in Oren et al's (1999) study. Such relatively high g_{sref} throughout a year were maintained by the availability of deep soil water, which, therefore, is thought to be a major cause for the high rubber E_T. It was found that g_{sref} reached an annual peak in JJA at Som Sanuk and in JJA to SON at CRRI. Further, it started to decrease at the withdrawal of the wet season, i.e., in SON at Som Sanuk and in DJF at CRRI (Fig. 7). Also, at both sites, g_{sref} reached its lowest point each year when $P - E_T < 0$, except for DJF 2010–2011 at CRRI when g_{sref} remained high. The process of full leaf-fall and full leaf-expansion was completed within the period of DJF, when $P - E_{T\_POT} < 0$.

Considering the above-mentioned behavior, rubber trees seem to avoid risk of water stress during the dry season by reducing activity, then maximizing activity when soil water is sufficient (see Kumagai and Porporato, 2012). The 0.6 proportionality (m/g_{sref})

was predicted from the examination of results of the plant transpiration model coupled with the hydraulic constraint model in which plants control transpiration rate via stomatal regulation to protect the transport system from excessive loss of hydraulic function (Oren et al., 1999; Cochard et al., 2002; Ewers et al., 2005; Katul et al., 2009). Thus, it was demonstrated that rubber trees maintained strict stomatal regulation to keep the difference between leaf water potential (ψ_L) and soil water potential constant in the period MAM 2010-JJA 2011 at CRRI. There was less sufficient stomatal regulation in the period SON 2011-DJF 2012 at CRRI and MAM 2009-SON 2010 at Som Sanuk (see Herbst et al., 2008; Kumagai et al., 2008; Naithani et al., 2012) (Fig. 8). Observations at CRRI showed somewhat constant midday ψ_L throughout the year, even in the dry season, partly confirming the strict stomatal regulation characteristics (data not shown here). Kumagai et al. (2008) hypothesized that the proportionality <0.6 for Japanese cedar would confer a carbon uptake advantage to tree species suitable for moist soil conditions, as there would be little risk of water stress-induced hydraulic failure and g_s would not have to decrease with increasing atmospheric demand. In this study, the proportionalities of ≈0.6 were realized at CRRI, where the ecosystem water resources were less than at Som Sanuk and the rubber trees had to extract water from the 0-3 m soil layer to compensate the water deficit under severe drought conditions (see Fig. 4). The values less than 0.6 were produced from somewhat moist conditions, such as the whole study period at Som Sanuk where there is more abundant precipitation, and the period SON 2011-DJF 2012 at CRRI, when the annual precipitation was about 200 mm higher than in 2010. These findings are consistent with the hypothesis of Kumagai et al. (2008).

In terms of regulation of water status, plants can be categorized as "isohydric" or "anisohydric" (see McDowell et al., 2008). Isohydric plants regulate transpiration by stomatal closure to maintain constant ψ_L, thus avoiding drought-induced hydraulic failure. In contrast, anisohydric plants have less stomatal sensitivity and allow ψ_L to decrease with decreasing soil moisture. On intra-annual time scales, the studied rubber trees had sensitive stomatal regulation under drought conditions, i.e., they exhibited isohydric behavior. However, anisohydric behavior was observed in the whole period at Som Sanuk and after SON 2011 at CRRI under moist environments where there was little risk of hydraulic failure (see Kumagai and Porporato, 2012). This alternating isohydric and anisohydric behavior makes these trees efficient in terms of water-use, as it allows the rubber trees to take advantage in their productivity under moist conditions and avoid risk of hydraulic failure under drought conditions.

5. Summary and implications

Results of this investigation suggest that for the rubber trees at Som Sanuk, where there is larger precipitation than at CRRI, water uptake from shallower soil depth and less stomatal regulation are sufficient under moist conditions, while at CRRI, the uptake from a deeper soil depth and strict stomatal regulation are necessary to cope with drier conditions. Because the studied sites are among the regions having the strongest seasonality in precipitation (see Kumagai et al., 2005), the strategy of these rubber trees for avoiding severe water stress in the dry season exhibits an exquisite balance between tree water use and the ecosystem water resource, which has drastic seasonal variation. This also means that there might be a "tipping point" (see Lenton et al., 2008) in the studied ecosystems, in that even a tiny perturbation in the ecosystem water resources via changes in rainfall regimes could alter their state, balance and development. For example, a close relationship between the interannual variations of the monsoon onset and El Niño-Southern Oscillation (ENSO) on the Indochina Peninsula was identified, and El Niño events appear to be associated with late monsoon onset leading to a reduction in annual precipitation (Zhang et al., 2002). Global warming is likely to cause changes in Pacific regional climate that might alter ENSO activity in the future (e.g., Timmermann et al., 1999). While it is still not clear how ENSO will be affected by global warming, it is possible that the frequency or amplitude of ENSO events could increase (Collins et al., 2010). Therefore, there is an urgent need to further examine the current and future perturbations in the hydrological, atmospheric and ecological processes responding to seasonal and interannual (e.g., ENSO-related) variation in precipitation in the region. One approach would be to combine an investigation of the impact of land use change (i.e., from pre-existing vegetation to rubber plantation; see Fig. 1; Fox et al., 2012) with this study's result of rubber plantations-atmosphere exchange characteristics.

Acknowledgements

The study in Cambodia was initiated as cooperative project between Cambodian Rubber Plantation Department, Cambodian Rubber Research Institute (CRRI), University of Hawai'i, and Kyushu University, supported by the Global COE (Centers of Excellence) Program (GCOE) of the Japan Society for the Promotion of Science (JSPS), National Aeronautics and Space Administration (NASA) grants NNG04GH59G and NNX08AL90G, and a grant from Kyushu University. We acknowledge help given by the staff of CRRI and other contributors, including Tsuyoshi Kajisa, Khun Kakada, Nobuya Mizoue, Makiko Tateishi, and Tetsukazu Yahara. TK, NK, and YM were supported by the project "Estimation and simulation of carbon stock change of tropical forest in Asia (2011–2014)" funded by the Ministry of Agriculture, Forestry and Fisheries, Japan. TK was supported by in part by a Grant-in-Aid for Scientific Research (# 23405028) and the granted project "Program for risk information on climate change" from the Ministry of Education, Science and Culture, Japan. MH was supported by the Office of Science of the U.S. Department of Energy (DOE) through the Earth System Modeling program. The Pacific Northwest National Laboratory (PNNL) is operated for the US DOE by Battelle Memorial Institute under contract DE-AC05-76RLO1830. Rubber mapping work was funded by NASA Earth System Science grants NNG04GH59G and NX08AL90G and the Geo-Informatics and Space Technology Development Agency of Thailand. ADZ was supported by National University of Singapore (NUS) grant R-109-000-092-133 and Asia-Pacific Network for Global Change Research (APN) grant #ARCP2008-01CMY.

References

Association of Natural Rubber Producing Countries (ANRPC), 2010. Natural Rubber Trends & Statistics Archive. Association of Natural Rubber Producing Countries (ANRPC), May http://www.anrpc.org/html/archive.aspx (29.0112. date last accessed).

Bréda, N.J.J., 2003. Ground-based measurements of leaf area index: a review of methods, instruments and current controversies. J. Exp. Bot. 54, 2403–2417.

Carr, M.K.V., 2012. The water relations of rubber (*Hevea brasiliensis*): a review. Exp. Agric. 48, 176–193.

Cochard, H., Coll, L., Roux, X.L., Amélio, T., 2002. Unraveling the effects of plant hydraulics on stomatal closure during water stress in walnut. Plant Physiol. 128, 282–290.

Collins, M., An, S.-I., Cai, W., Ganachaud, A., Guilyardi, E., Jin, F.-F., Jochum, M., Lengaigne, M., Power, S., Timmermann, A., Vecchi, G., Wittenberg, A., 2010. The impact of global warming on the tropical Pacific Ocean and El Niño. Nat. Geosci. 3, 391–397.

Delzon, S., Sartore, M., Burlett, R., Dewar, R., Loustau, D., 2004. Hydraulic responses to height growth in maritime pine trees. Plant Cell Environ. 27, 1077–1087.

Ewers, B.E., Oren, R., 2000. Analyses of assumptions and errors in the calculation of stomatal conductance from sap flux measurements. Tree Physiol. 20, 579–589.

Ewers, B.E., Oren, R., Phillips, N., Strögren, M., Linder, S., 2001. Mean canopy stomatal conductance responses to water and nutrient availabilities in *Picea abies* and *Pinus taeda*. Tree Physiol. 21, 841–850.
Ewers, B.E., Gower, S.T., Bond-Lamberty, B., Wang, C.K., 2005. Effects of stand age and tree species on canopy transpiration and average stomatal conductance of boreal forests. Plant Cell Environ. 28, 660–678.
Ewers, B.E., Mackay, D.S., Samanta, S., 2007. Interannual consistency in canopy stomatal conductance control of leaf water potential across seven tree species. Tree Physiol. 27, 11–24.
Fox, J., Vogler, J.B., Sen, O.L., Giambelluca, T.W., Ziegler, A.D., 2012. Simulating land-cover change in montane mainland Southeast Asia. Environ. Manage. 49, 968–979.
Fox, J.M., Castella, J.-C., Ziegler, A.D., Westley, S.B., 2014. Rubber Plantations Expand in Mountainous Southeast Asia: What Are the Consequences for the Environment? AsiaPacific Issues, Analysis from the East-West Center No. 114. East-West Center, Honolulu, May.
Giambelluca, T.W., Mudd, R.G., Liu, W., Ziegler, A.D., Kobayashi, N., Kumagai, T., Miyazawa, Y., Lim, T.K., Huang, M., Fox, J., Yin, S., Mak, S.V., Kasemsap, P., 2015. Evapotranspiration of rubber (*Hevea brasiliensis*) cultivated at two sites in southeast Asia. Water Resour. Res., submitted for publication.
Guardiola-Claramonte, M., Troch, P.A., Ziegler, A.D., Giambelluca, T.W., Vogler, J.B., Nullet, M.A., 2008. Local hydrologic effects of non-native vegetation in a tropical catchment. Ecohydrology 1, 13–22.
Guardiola-Claramonte, M., Troch, P.A., Ziegler, A.D., Giambelluca, T.W., Durcik, M., Vogler, J.B., Nullet, M.A., 2010. Hydrologic effects of the expansion of rubber (*Hevea brasiliensis*) in a tropical catchment. Ecohydrology 3, 306–314.
Herbst, M., Rosier, P.T.W., Morecroft, M.D., Gowing, D.J., 2008. Comparative measurements of transpiration and canopy conductance in two mixed deciduous woodlands differing in structure and species composition. Tree Physiol. 28, 959–970.
Isarangkool Na Ayutthaya, S., Do, F.C., Pannangpetch, K., Junjittakarn, J., Maeght, J.-L., Rochetau, A., Cochard, H., 2011. Water loss regulation in mature *Heavea brasiliensis*: effects of intermittent drought in the rainy season and hydraulic regulation. Tree Physiol. 31, 751–762.
Jackson, R.B., Canadell, J., Ehleringer, J.R., Mooney, H.A., Sala, O.E., Schulze, E.D., 1996. A global analysis of root distributions for terrestrial biomes. Oecologia 108, 389–411.
Jarvis, P.G., 1976. The interpretation of the variations in leaf water potential and stomatal conductance found in canopies in the field. Philos. Trans. R. Soc. Lond. Biol. 273, 593–610.
Katul, G.G., Palmroth, S., Oren, R., 2009. Leaf stomatal responses to vapour pressure deficit under current and CO_2-enriched atmosphere explained by the economics of gas exchange. Plant Cell Environ. 32, 968–979.
Kelliher, F.M., Luening, R., Raupach, M.R., Schulze, E.-D., 1995. Maximum conductances for evaporation from global vegetation types. Agric. For. Meteorol. 73, 1–16.
Kitajima, K., Mulkey, S.S., Samaniego, M., Wright, J.S., 2002. Decline of photosynthetic capacity with leaf age and position in two tropical pioneer tree species. Am. J. Bot. 89, 1925–1932.
Kobayashi, N., Kumagai, T., Miyazawa, Y., Matsumoto, K., Tateishi, M., Lim, T.K., Mudd, R.G., Ziegler, A.D., Giambelluca, T.W., Yin, S., 2014. Transpiration characteristics of a rubber plantation in central Cambodia. Tree Physiol. 34, 285–301.
Kucharik, C.J., Norman, J.M., Gower, S.T., 1998. Measurements of branch area and adjusting leaf area index indirect measurements. Agric. For. Meteorol. 91, 69–88.
Kumagai, T., Porporato, A., 2012. Strategies of a Bornean tropical rainforest water use as a function of rainfall regime: isohydric or anisohydric? Plant Cell Environ. 35, 61–71.
Kumagai, T., Saitoh, T.M., Sato, Y., Morooka, T., Manfroi, O.J., Kuraji, K., Suzuki, M., 2004. Transpiration, canopy conductance and the decoupling coefficient of a lowland mixed dipterocarp forest in Sarawak, Borneo: dry spell effects. J. Hydrol. 287, 237–251.
Kumagai, T., Saitoh, T.M., Sato, Y., Takahashi, H., Manfroi, O.J., Morooka, T., Kuraji, K., Suzuki, M., Yasunari, T., Komatsu, H., 2005. Annual water balance and seasonality of evapotranspiration in a Bornean tropical rainforest. Agric. For. Meteorol. 128, 81–92.
Kumagai, T., Aoki, S., Shimizu, T., Otsuki, K., 2008. Transpiration and canopy conductance at two slope positions in a Japanese cedar forest watershed. Agric. For. Meteorol. 148, 1444–1455.
Kumagai, T., Aoki, S., Otsuki, K., Utsumi, Y., 2009a. Impact of stem water storage on diurnal estimates of whole-tree transpiration and canopy conductance from sap flow measurements in Japanese cedar and Japanese cypress. Hydrol. Process. 23, 2335–2344.
Kumagai, T., Yoshifuji, N., Tanaka, N., Suzuki, M., Kume, T., 2009b. Comparison of soil moisture dynamics between a tropical rainforest and a tropical seasonal forest in Southeast Asia: impact of seasonal and year-to-year variations in rainfall. Water Resour. Res. 45, W04413, http://dx.doi.org/10.1029/2008WR007307
Kumagai, T., Mudd, R.G., Miyazawa, Y., Liu, W., Giambelluca, T.W., Kobayashi, N., Lim, T.K., Jomura, M., Matsumoto, K., Huang, M., Chen, Q., Ziegler, A., Yin, S., 2013. Simulation of canopy CO_2/H_2O fluxes for a rubber (*Hevea brasiliensis*) plantation in central Cambodia: the effect of the regular spacing of planted trees. Ecol. Model. 265, 124–135.
Kumagai, T., 2011. Transpiration in forest ecosystems. In: Levia, D.F., Carlyle-Moses, D., Tanaka, T. (Eds.), Forest Hydrology and Biogeochemistry: Synthesis of Past Research and Future Directions, Ecological Studies 216. Springer, New York, pp. 389–406.
Lenton, T.M., Held, H., Kriegler, E., Hall, J.W., Lucht, W., Rahmstorf, S., Schellnhuber, H.J., 2008. Tipping elements in the Earth's climate system. Proc. Natl. Acad. Sci. U. S. A. 105, 1786–1793.
Li, Z., Fox, J., 2011. Mapping rubber tree growth in mainland Southeast Asia using time-series MODIS 250m NDVI and statistical data. Appl. Geogr. 32, 420–432.
Mann, C.C., 2009. Addicted to rubber. Science 325, 564–566.
Markewitz, D., Devine, S., Davidson, E.A., Brando, P., Nepstad, D.C., 2010. Soil moisture depletion under simulated drought in the Amazon: impacts on deep root uptake. New Phytol. 187, 592–607.
McDowell, N., Pockman, W.T., Allen, C.D., Breshears, D.D., Cobb, N., Kolb, T., Plaut, J., Sperry, J., West, A., Williams, D.G., Yepez, E.A., 2008. Mechanisms of plant survival and mortality during drought: why do some plants survive while others succumb to drought? New Phytol. 178, 719–739.
Naithani, K.J., Ewers, B.E., Pendall, E., 2012. Sap flux-scaled transpiration and stomatal conductance response to soil and atmospheric drought in a semi-arid sagebrush ecosystem. J. Hydrol. 464–465, 176–185.
Nepstad, D.C., de Carvalho, C.R., Davidson, E.A., Jipp, P.H., Lefebvre, P.A., Negreiros, G.H., da Silva, E.D., Stone, T.A., Trumbore, S.E., Vieira, S., 1994. The role of deep roots in the hydrological and carbon cycles of Amazonian forests and pastures. Nature 372, 666–669.
Oren, R., Sperry, J.S., Katul, G.G., Pataki, D.E., Ewers, B.E., Phillips, N., Schäer, K.V.R., 1999. Survey and synthesis of intra- and interspecific variation in stomatal sensitivity to vapour pressure deficit. Plant Cell Environ. 22, 1515–1526.
Pataki, D.E., Oren, R., 2003. Species differences in stomatal control of water loss at the canopy scale in a mature bottomland deciduous forest. Adv. Water Resour. 26, 1267–1278.
Pokorný, R., Marek, M.V., 2000. Test of accuracy of LAI estimation by LAI-2000 under artificially changed leaf to wood area proportions. Biol. Plant 43, 537–544.
Priestley, C.H.B., Taylor, R.J., 1972. On the assessment of surface heat flux and evaporation using large-scale parameters. Mon. Weather Rev. 100, 81–92.
Priyadarshan, P.M., Hoa, T.T.T., Huasun, H., Goncalves, P.d.S., 2005. Yielding potential of rubber (*Hevea brasiliensis*) in sub-optimal environments. In: Kang, M.S. (Ed.), Genetic and Production Innovations in Field Crop Technology: New Development in Theory and Practice. The Haworth Press Inc., Philadelphia, pp. 221–247.
Priyadarshan, P.M., 2003. Breeding *Hevea brasiliensis* for environmental constraints. Adv. Agron. 79, 351–400.
Qiu, J., 2009. Where the rubber meets the garden. Nature 457, 246–247.
Raupach, M., Finnigan, J., 1988. 'Single-layer models of evaporation from plant canopies are incorrect but useful, whereas multilayer models are correct but useless. Discuss. Aust. J. Plant Physiol. 15, 705–716.
Sangsing, K., Kasemsap, P., Thanisawanyangkura, S., Sangkhasila, K., Gohet, E., Thaler, P., Cochard, H., 2004. Xylem embolism and stomatal regulation in two rubber clones (*Hevea brasiliensis* Muell. Arg.). Trees 18, 109–114.
Schäer, K.V.R., Oren, R., Tenhunen, J.D., 2000. The effect of tree height on crown level stomatal conductance. Plant Cell Environ. 23, 365–375.
Schmidt-Walter, P., Richter, F., Herbst, M., Schuldt, B., Lamersdorf, P, 2014. Transpiration and water use strategies of a young and a full-grown short rotation coppice differing in canopy cover and leaf area. Agric. For. Meteorol. 195, 165–178.
Stahl, C., Herault, B., Rossi, V., Burban, B., Brechet, C., Bonal, D., 2013. Depth of soil water uptake by tropical rainforest trees during dry periods: does tree dimension matter. Oecologia 173, 1191–1201.
Tan, Z.-H., Zhang, Y.-P., Song, Q.-H., Liu, W.-J., Deng, X.-B., Tang, J.-W., Deng, Y., Zhou, W.-J., Yang, L.-Y., Yu, G.-R., Sun, X.-M., Liang, N.-S., 2011. Rubber plantations act as water pumps in tropical China. Geophys. Res. Lett. 38, L2440, http://dx.doi.org/10.1029/2011GL050006
Tateishi, M., Kumagai, T., Suyama, Y., Hiura, T., 2010. Differences in transpiraton characteristics of Japanese beech trees, *Fagus crenata*, in Japan. Tree Physiol. 30, 748–760.
Timmermann, A., Oberhuber, J., Bacher, A., Esch, M., Latif, M., Roeckner, E., 1999. Increased El Niño frequency in a climate model forced by future greenhouse warming. Nature 398, 694–697.
Wang, B., LinHo, 2002. Rainy season of the Asian-Pacific summer monsoon. J. Clim. 15, 386–398.
Wauters, J.B., Coudert, S., Grallien, E., Jonard, M., Ponette, Q., 2008. Carbon stock in rubber tree plantations in Western Ghana and Mato Grosso (Brazil). For. Ecol. Manage. 255, 2347–2361.
Wilson, K.B., Baldocchi, D.D., Hanson, P.J., 2001. Leaf age affects the seasonal pattern of photosynthetic capacity and net ecosystem exchange of carbon in a deciduous forest. Plant Cell Environ. 24, 571–583.
Wu, Z.-L., Liu, H.-M., Liu, L.-Y., 2001. Rubber cultivation and sustainable development in Xishuangbanna, China. Int. J. Sustain. Dev. World Ecol. 8, 337–345.
Wullschleger, S.D., Wilson, K.B., Hanson, P.J., 2000. Environmental control of whole-plant transpiration, canopy conductance and estimates of the decoupling coefficient for large red maple trees. Agric. For. Meteorol. 104, 157–168.
Zhang, Y., Li, T., Wang, B., Wu, G., 2002. Onset of the summer monsoon over the Indochina Peninsula: climatology and interannual variations. J. Clim. 15, 3206–3221.

Ziegler, A.D., Bruun, T.B., Guardiola-Claramonte, M., Giambelluca, T.W., Lawrence, D., Nguyen, T.L., 2009a. Environmental consequences of the demise in swidden agriculture in SE Asia: hydrology and geomorphology. Hum. Ecol. 37, 361–373.
Ziegler, A.D., Fox, J.M., Xu, J., 2009b. The rubber juggernaut. Science 324, 1024–1025.
Ziegler, A.D., Phelps, J., Yuen, J.Q., Webb, E.L., Lawrence, D., Fox, J.M., Bruun, T.B., Leisz, S.J., Ryan, C.M., Dressler, W., Mertz, O., Pascual, U., Padoch, C., Koh, L.P., 2012. Carbon outcomes of major land-cover transitions in SE Asia: great uncertainties and REDD+ policy implications. Glob. Change Biol. 18, 3087–3099.